RSC Advances

PAPER

View Article Online
View Journal | View Issue

Check for updates

Cite this: *RSC Adv.*, 2022, **12**, 5072

Enzyme-free glucose sensors with efficient synergistic electro-catalysis based on a ferrocene derivative and two metal nanoparticles†

Tao Zhan,‡[ab] Xiao-Zhen Feng,‡[b] Qi-Qi An,‡[b] Shiyong Li,[a] Mingyue Xue,[b] Zhencheng Chen,*[ab] Guo-Cheng Han*[b] and Heinz-Bernhard Kraatz*[c]

Received 20th December 2021
Accepted 25th January 2022

DOI: 10.1039/d1ra09213h

rsc.li/rsc-advances

Gold electrodes (GE) were modified by the deposition of copper nanoparticles (CuNPs) and cobalt nanoparticles (CoNPs), followed by drop-casting of the ferrocene derivative FcCO-Glu-Cys-Gly-OH (Fc-ECG), resulting in two enzyme-free electrochemical sensors Fc-ECG/CuNPs/GE and Fc-ECG/CuNPs/GE. The ferrocene-peptide conjugate acts as an effective redox mediator for glucose oxidation, while metal nanoparticles acted as non-biological sites for glucose oxidation. Field emission scanning electron microscopy (FESEM), cyclic voltammetry (CV) and electrochemical impedance spectroscopy (EIS) were carried out for characterization, while differential pulse voltammetry (DPV) was used for glucose quantification. Under optimized conditions, DPV shows a linear relationship between glucose concentration and the peak current. Both sensors showed a surprisingly high sensitivity of 217.27 and 378.70 μA mM^{-1} cm^{-2}, respectively. A comparison to other glucose sensors shows a sensitivity that is 25 times higher. The sensors exhibit good reproducibility, stability, and repeatability. In injection experiments, recovery rates were 87.39–107.65% and 100.00–106.88%, respectively.

1. Introduction

Diabetes has become a worldwide problem especially in low- and middle-income countries. According to the global report on diabetes[1] from the World Health Organization (WHO) in 2016, the prevalence of diabetes has been steadily increasing for the past three decades. There were 422 million cases counted in 2014 alone, which is even far more than was predicted by Wild *et al.*[2] Monitoring glucose levels in those affected by diabetes is critical for managing the disease.[3] The earliest enzyme-based glucose sensor was developed by Clark and Lyons.[4] And there has been a steady development of new electrochemical glucose sensors, largely by allowing the determination of blood glucose concentrations exploiting the catalytic function of glucose oxidase (GOx) or glucose dehydrogenase (GDH).[5,6] Enzymatic glucose sensors have been successfully commercialized and are based on key contributions by Turner and others,[7] who advanced the use of redox mediators like ferrocene derivatives in enzymatic glucose detection. However, the performance of enzymatic sensors is closely related to the stability and bioactivity of the redox enzyme that is part of the sensor, which is often strongly affected by environmental factors, including temperature and pH. Thus enzyme-free glucose biosensors, the fourth generation of glucose biosensors, have attracted increasing attention as they would not suffer from such drawbacks.[8,9]

Non-enzymatic glucose sensors usually use modified electrode materials as electrocatalysts in alkaline solution.[10,11] Precious metals (Au, Ag and Pt),[12,13] transition metals (Fe, Cu, Co, Ni and Pd)[14–16] as well as their oxides,[17,18] and metal–organic framework-based materials[19] are most commonly used to electrochemically catalyze glucose to glucolactone, followed by hydrolysis to gluconic acid or gluconate. Such sensors are often more stable and provide reproducible results, while at the same time are more cost effective and easier to store, due to the absence of enzymes. However, many also suffer from low sensitivity and a narrow linear range. In addition, their function is limited to a strong alkaline environment (usually pH 13.0).[20,21] At present, a considerable number of innovative nanostructures have been reported to improve on these obvious drawbacks and enhance the sensitivity of the sensor systems and render then useable under physiological conditions.[13,22] And part of this development is the push for applications of smart sensors in intelligent wear, sensing human health by detecting the glucose content in sweat.[23] Ferrocene is a widely used redox electronic medium which can accelerate

[a]*College of Electronic Engineering and Automation, Guilin University of Electronic Technology, Guilin 541004, P. R. China. E-mail: chenzhch1965@163.com*

[b]*School of Life and Environmental Sciences, Guilin University of Electronic Technology, Guilin 541004, P. R. China. E-mail: hangc81@guet.edu.cn*

[c]*Department of Physical and Environmental Sciences, University of Toronto Scarborough, Toronto, Ontario M1C 1A4, Canada. E-mail: bernie.kraatz@utoronto.ca*

† Electronic supplementary information (ESI) available. See DOI: 10.1039/d1ra09213h

‡ These authors contributed equally to the work.

Open Access Article. Published on 10 February 2022. Downloaded on 2/15/2026 8:42:09 PM. This article is licensed under a Creative Commons Attribution-NonCommercial 3.0 Unported Licence.

© 2022 The Author(s). Published by the Royal Society of Chemistry

Open Access Article. Published on 10 February 2022. Downloaded on 2/15/2026 8:42:09 PM.
This article is licensed under a Creative Commons Attribution-NonCommercial 3.0 Unported Licence.

electron transfer and catalytic reaction in electrochemical reaction.[24,25] Substituted ferrocene derivatives are particularly useful in this context as substituents can enhance the electron donor ability of ferrocene.[26,27] An example is ferrocene covalently linked to glutathione, which has advantages of multiple active binding sites and good biocompatibility.[28,29] Over the past few years, our group has successfully constructed several high-performance sensors using the ferrocene–glutathione conjugate Fc[CO-Glu-Cys-Gly-OH] (Fc-ECG).[30,31] And while ferrocene derivatives have long been used in enzyme-based electrochemical glucose sensors, but are relatively less applied to enzyme-free glucose sensors.[32,33]

In this work, we exploit the ferrocene-glutathione conjugate Fc-ECG as electron transfer mediator and make use of gold electrodes that were modified with either copper nanoparticles (CuNPs) or cobalt nanoparticles (CoNPs) to give sensor surfaces that exhibit excellent catalytic activity of glucose oxidation. Electrochemical methods, including cyclic voltammetry (CV), differential pulse voltammetry (DPV) and electrochemical impedance spectroscopy (EIS), were used to study the electrochemical performance of the modified electrodes. In addition, the surfaces were fully characterized by field emission scanning electron microscopy (FESEM) and energy dispersive spectroscopy (EDS) that allowed us to characterize surface morphologies for each of the modification steps. The sensor systems described in this contribution exhibit wide linear ranges and high sensitivities for glucose detection, while showing a good reproducibility, repeatability, stability, and selectivity.

2. Experimental section

2.1 Reagents and apparatus

Glucose (99% purity) was obtained from Shanghai Aladdin Biochemical Technology Co., Ltd and used as received. Glucose injections were purchased from Hubei Kelun Pharmaceutical Co., Ltd. Fc[CO-Glu-Cys-Gly-OH] (Fc-ECG) was produced by Xi'an Chemical Reagent Factory. Copper sulfate ($CuSO_4 \cdot 5H_2O$) was purchased from Xilong Science Co., Ltd. Cobalt chloride ($CoCl_2 \cdot 6H_2O$) was purchased from Guangdong Province Chemical Reagent Engineering Technology Research and Development Center. Folic acid (FA) was obtained from Nanjing Chemical Reagent Co., Ltd. β-Cyclodextrin (β-CD) was purchased from Shanghai Yuanye Biotechnology Co., Ltd. Dopamine (DA) and ascorbic acid (AA) were obtained from the Shanghai Reagent Factory. Phosphate buffer solution (PBS) was prepared from NaH_2PO_4 and Na_2HPO_4 and the pH was adjusted. All aqueous solutions in the experiments were prepared with ultra-pure (UP) water and all other reagents were analytically pure.

Cyclic voltammetry (CV), differential pulse voltammetry (DPV), amperometric *i–t* measurements (*i–t*) and electrochemical impedance spectroscopy (EIS) experiments were performed on the CHI660E electrochemical workstation (Shanghai Chenhua Instrument Co., Ltd, Shanghai, China) controlled from a computer and equipped with a conventional three-electrode system, consisting of an Ag/AgCl (with saturated KCl) as the reference electrode, a platinum wire as the counter electrode and GE as the working electrode ($\varphi = 0.3$ cm). In the electrochemical glucose detection experiments 0.1 M NaOH solution was used as the electrolyte. Morphologies and elemental composition of all samples were characterized by field emission scanning electron microscope (FESEM, Hitachi SU8020 from Japan) with a resolution of 1.0 nm and an element range of B5-U92.

2.2 Modification gold electrodes to form Fc-ECG/CuNPs/GE and Fc-ECG/CoNPs/GE

Prior to modification, the gold electrodes were polished and then rinsed with ethanol, followed by rinsing with UP water. Then CuNPs were deposited onto the surface of GE by *i–t* at −0.37 V for 180 s in a mixed solution of 0.1 M $CuSO_4$ and 0.1 M H_2SO_4. Similarly, CoNPs was deposited on GE *via* CV with a scan

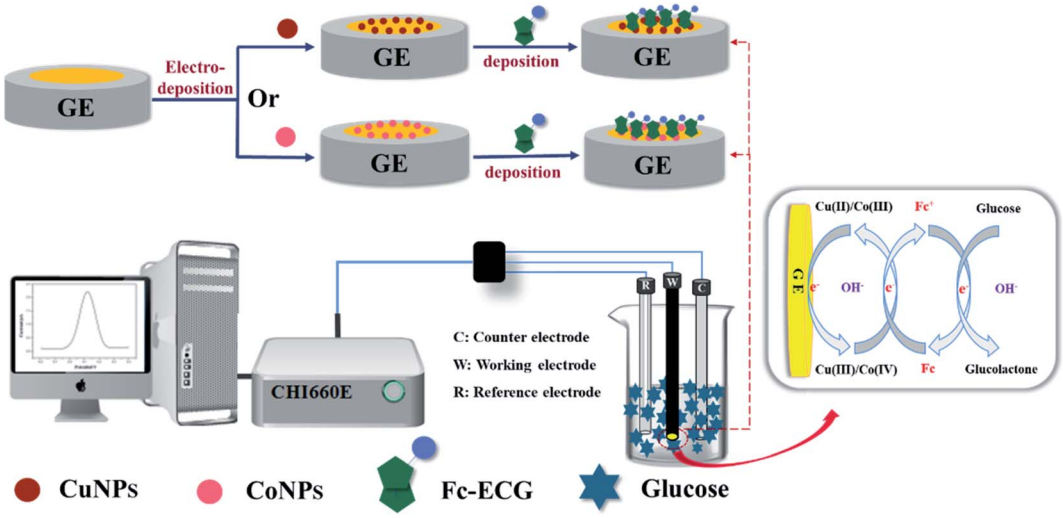

Scheme 1 Preparation of Fc-ECG/CuNPs/GE and Fc-ECG/CoNPs/GE sensors for glucose detection by DPV technique in alkaline solution.

Open Access Article. Published on 10 February 2022. Downloaded on 2/15/2026 8:42:09 PM.
This article is licensed under a Creative Commons Attribution-NonCommercial 3.0 Unported Licence.

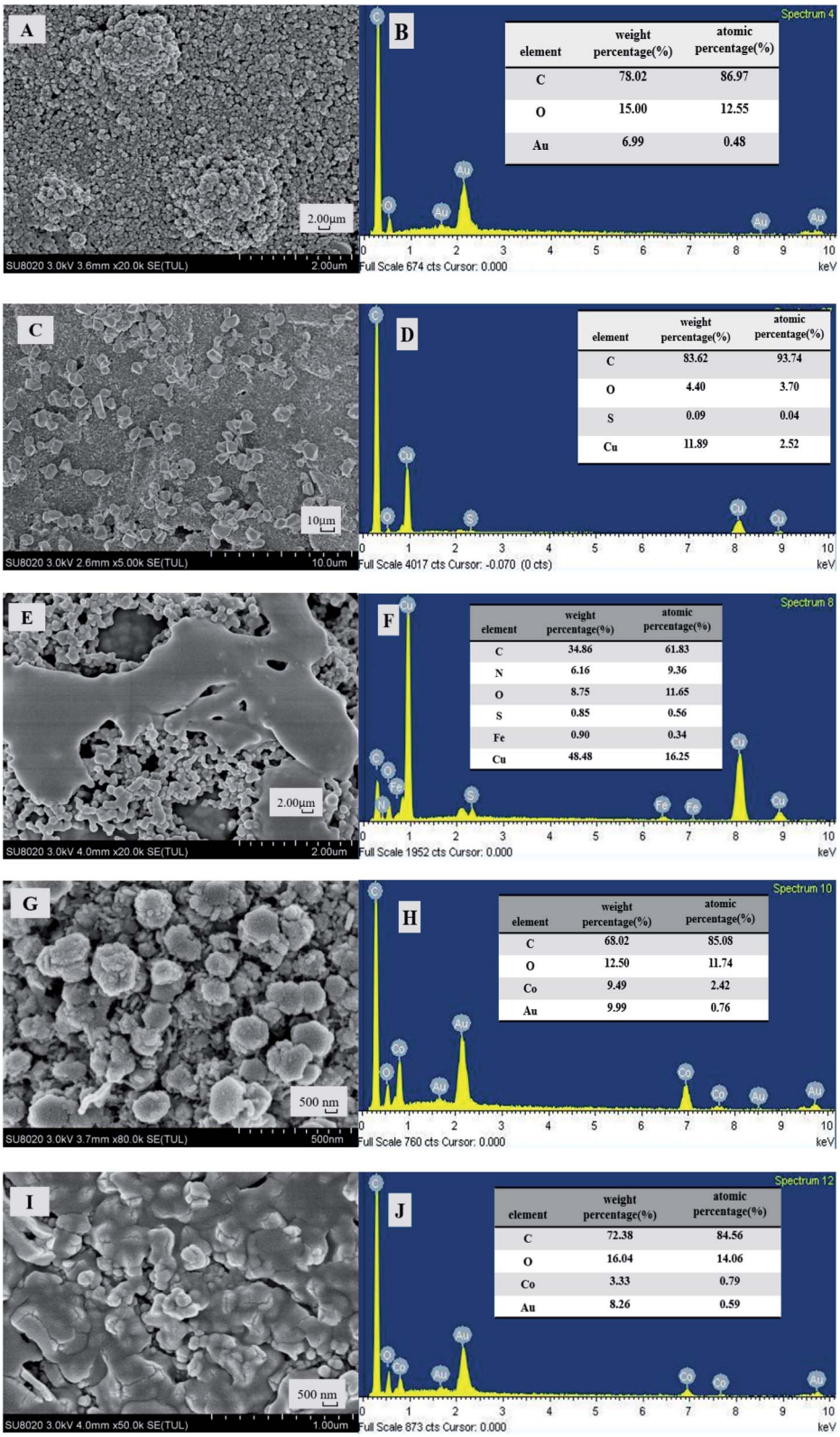

Fig. 1 SEM (left) and EDS (right) characterization of the prepared electrodes. (A and B) Screen printing electrode with gold deposited; (C and D) CuNPs/GE; (E and F) Fc-ECG/CuNPs/GE; (G and H) CoNPs/GE; (I and J) Fc-ECG/CoNPs/GE.

interval from −1.10 to −0.68 V for 5 circles in 0.01 M $CoCl_2$. Finally, Fc-ECG was dropped on the modified GE with 0.50 mM Fc-ECG (dissolved in water with the help of acetonitrile) and dried in air. Thus Fc-ECG/CuNPs/GE and Fc-ECG/CoNPs/GE were obtained. The synthetic approach is illustrated in Scheme 1.

© 2022 The Author(s). Published by the Royal Society of Chemistry

Open Access Article. Published on 10 February 2022. Downloaded on 2/15/2026 8:42:09 PM.
This article is licensed under a Creative Commons Attribution-NonCommercial 3.0 Unported Licence.

3. Results and discussion

3.1 Characterization of the modified electrodes

The morphologies and elemental composition of the modified electrode Fc-ECG/CuNPs/GE and Fc-ECG/CoNPs/GE have been investigated by FESEM with scanning electron microscopy (SEM) and X-ray energy dispersion spectroscopy (EDS). For ease of investigation, screen printed gold electrodes were used for this purpose. Fig. 1 shows the results of the SEM and EDS studies of the two electrode surfaces.

Fig. 1A shows a bare screen printed gold electrode and the EDS analysis (Fig. 1B) shows the presence of Au. After modification with CuNPs, irregular crystallites are visible on the surface (Fig. 1C), and the corresponding EDS image (Fig. 1D) shows the presence of Cu on the surface. Drop-casting Fc-ECG, alters the surface morphology of the surface and the presence of Fe (Fig. 1E and F) as a result of ferrocene-peptide deposition demonstrates the successful modification of Fc-ECG. Likewise, CoNP modification is shown in Fig. 1G and H, and Fig. 1I and J show the presence of CoNPs and Fc-ECG.

CV and EIS experiments were carried out to characterize the modified electrode surfaces for each of the modification steps. The results of this study are shown in Fig. S1.† Fig S1A and B† show the CV curves of different electrodes in PBS (pH = 7.0) and the EIS curves are shown in Fig. S1C and D.†

As is expected, the bare gold electrode exhibits no electrocatalytic activity in PBS. But as the electrode is modified with CuNPs or CoNPs and then with Fc-ECG, new faradaic features are visible (see Fig S1A and B,† curves b and c). Further characterization of the electrode surfaces using electrochemical impedance spectroscopy (EIS) allows to gain more information about the electron transfer properties of the two different electrode surfaces. Fig. 1C and D show the results of our EIS study in the form of Nyquist plots, from which the electron transfer resistance (R_{ct}) can be obtained with the help of an equivalent circuit. Visually, the semi-circle related to R_{ct},[34,35] GE has a small impedance that was reduced by the deposited CoNPs, which is opposite to the result of CoNPs, then Fc-ECG also changed the impedance of the modified electrode surface. Glucose, afterwards, increased the impedance of two proposed sensor.

3.2 Electrocatalytic performance of the surfaces in glucose solution

Fig. S2† describes the electrocatalytic properties of Fc-ECG/CuNPs/GE and Fc-ECG/CoNPs/GE in the presence of glucose (4 mM glucose and 0.1 M NaOH). As shown in Fig. S2A and B,† curve a is considered as a baseline as no obvious peak can be observed on glassy carbon electrode (GCE) when tested in glucose. It can be seen that CuNPs or CoNPs on the surface of GE have a strong catalytic effect on the oxidation of glucose which is likely to be generated by the redox pairs couples Cu(II)/Cu(III), Co(III)/Co(IV) under alkaline conditions.[18] Moreover, the modified Fc-ECG, as an effective redox reaction mediator, accelerates the electron transfer between them resulting in the significant amplification of the response current.[36] The possible reaction mechanism is shown in Scheme 1. Both Fc-ECG/CuNPs/GE and Fc-ECG/CoNPs/GE are feasible for glucose detection and the latter has the stronger electrochemical response.

3.3 Optimization studies

Next, the optimization of the experimental conditions was performed. Parameters to be considered include pH, amount of Fc-ECG modification, temperature, *i*–*t* deposition time of CuNPs, and the number of CV scans for deposition of CoNPs. The responses of the surfaces to change in these parameters are shown in Fig. S3A–E.† Fig. S3A† shows no influence of pH on the electrochemical response at pH values below pH 13.0. Thus, we chose strong alkaline conditions for our experiments. This is also consistent with other reports showing the need to alkaline conditions.[20,21] Fig. S3B† shows maximum peak current responses for Fc-ECG/CuNPs/GE and Fc-ECG/CoNPs/GE at 25 °C. Fig. S3C,† DPV response of Fc-ECG/CuNPs/GE and Fc-ECG/CuNPs/GE reached the maximum value when 5 and 6 μL Fc-ECG was dropped onto the electrodes, respectively. Considering that the responses were very similar, it was decided to continue with a deposition of 5 μL of Fc-ECG solution. Next, the conditions for NP depositions were tested. Fig. S3D† indicates that the largest peak response was obtained at a deposition time of 180 s for CuNPs. While for CoNPs the optimal conditions were obtained after 5 CV cycles (Fig. S3E†).

3.4 Glucose detection assays

Next in our study, we evaluated the electrochemical responses of the Fc-ECG/CuNPs/GE and Fc-ECG/CoNPs/GE sensor surfaces at optimized conditions to various glucose concentrations in 0.1 M NaOH solution (see Fig. 2A and B).

DPV curves showed in Fig. 2 reveal that the oxidation current (I, μA) of glucose at both sensors increases with increasing glucose concentration (c, mM) and has excellent linear relationships. The glucose oxidation current on Fc-ECG/CuNPs/GE is proportional to glucose concentration from 0.40 to 2.30 mM (Fig. 2A). The linear regression equation is $I = 1.69792 + 15.35783c$ ($R^2 = 0.99196$). The detection limit of proposed Fc-ECG/CuNPs/GE is calculated as 0.13 mM (S/N = 3) and the sensitivity is 217.27 μA mM^{-1} cm^{-2}. Fig. 2B illustrates the DPV curves obtained from Fc-ECG/CoNPs/GE (the inset shows a good linear relationship between the glucose concentration and the peak current), the linear regression equation is $I = 8.65946 + 26.76856c$ ($R^2 = 0.99627$). A sensitivity of 378.70 μA mM^{-1} cm^{-2} and a detection limit of 0.23 mM (S/N = 3) were obtained. Obviously, Fc-ECG/CoNPs/GE exhibits a higher sensitivity and wider linear range. The electrochemical responses exhibit a linear range and sensitivity that compares well to glucose sensors reported previously and listed in Table 1.

3.5 Selectivity, stability, reproductivity and repeatability

For the next set of experiments, *i*–*t* measurements were carried out to evaluate the stability and the selectivity of the Fc-ECG/

Open Access Article. Published on 10 February 2022. Downloaded on 2/15/2026 8:42:09 PM.
This article is licensed under a Creative Commons Attribution-NonCommercial 3.0 Unported Licence.

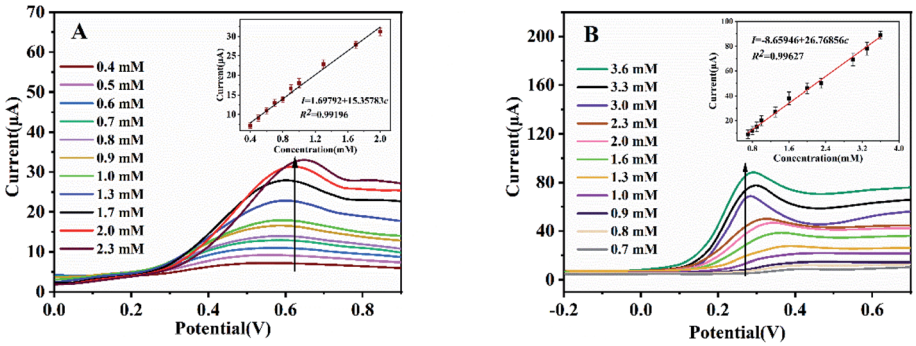

Fig. 2 (A) DPVs of Fc-ECG/CuNPs/GE in mixed solution of 0.1 M NaOH and different concentrations (0.40–2.30 mM) glucose, inset: calibration plots for various concentrations of glucose; (B) DPVs of Fc-ECG/CuNPs/GE in mixed solution of 0.1 M NaOH and different concentrations (0.70–3.60 mM) glucose, inset: calibration plots for various concentrations of glucose.

Table 1 Performance comparison of various glucose sensors

Sensors	Linear ranges (mM)	Sensitivity ($\mu A\ mM^{-1}\ cm^{-2}$)	Reference
NPGWE	0.50–10.00	128.80	37
PAA-VS-PANI/GPL-FePc/GOx-CH	1.00–20.00	18.11	38
PAA-rGO/VS-PANI/LuPc$_2$/GOx-MFH	2.00–12.00	15.31	39
Cu/Cu$_2$O nanoporous NPs	0.01–5.50	123.80	40
PdNS-Cu/Cu$_2$O/FTO	0.0005–2.60	—	41
AuNPs@CuO NWs/Cu$_2$O/CF	0.0028–2.00	1.62	42
NiCo-LDH/CCCH/CuF	0.001–1.50	10.78	43
Fc-ECG/CuNPs/GE	0.40–2.30	217.27	This work
Fc-ECG/CoNPs/GE	0.70–3.60	378.70	This work

CuNPs/GE and Fc-ECG/CoNPs/GE were studied (Fig. 3A). To verify the stability of prepared sensors, glucose was detected by two sensors every 5 min continuously for three times (Fig. 3B). For repeatability study, studies were carried out on four different electrodes. The peak current response for the four electrodes is shown in Fig. 3C (the inset were DPVs). More broadly, the reproducibility of two constructed sensors was studied by measuring consecutive samples of the same concentration, and the results are illustrated in Fig. 3D (the inset are the DPV responses for the individual measurements).

As can be seen form line a in Fig. 3A, current responses from the Fc-ECG/CoNPs/GE were generated when 10 mM glucose were added dropwise at 100, 150, 400, 500 s. The electrochemical response to glucose addition of the Fc-ECG/CuNPs/GE surface is shown in line b. Importantly, the addition of potential interferents (1.00 mM FA, 10.00 mM β-CD, 0.01 mM DA, 0.50 mM AA 1.00 mM NaCl and 20.00 mM $NaNO_3$) does not cause any significant changes in the electrochemical response. The experimental data shown in Fig. 3B (the insets are corresponding DPVs) indicates that the peak current value of Fc-ECG/CuNPs/GE and Fc-ECG/CoNPs/GE was 4.63 ± 0.28 μA (RSD = 4.30%) and 87.66 ± 2.10 μA (RSD = 2.23%), respectively. From the experimental data in Fig. 3C, when the electrochemical responses from four different electrodes gives measured peak current values for Fc-ECG/CuNPs/GE and Fc-ECG/CoNPs/GE of 40.18 ± 4.00 μA (RSD = 3.16%) and 68.48 ± 4.14 μA (RSD = 6.44%), respectively, indicating consistency and repeatability of the measurements. Moreover, when four separate measurements are made with one electrode, the peak current values of Fc-ECG/CuNPs/GE and Fc-ECG/CoNPs/GE were 4.65 ± 0.15 μA (RSD = 2.23%) and 87.66 ± 2.10 μA (RSD = 2.23%), respectively (Fig. 3D).

3.6 Analysis of real sample

Finally, Fc-ECG/CoNPs/GE and Fc-ECG/CoNPs/GE sensors were used to detect the concentration of glucose in glucose injection to investigate the feasibility of practical applications. In this experiment, 4 mL glucose injection with a diluted concentration of 1.30 mM with 1 mL NaOH added was drew to be tested for three times. According to the linear equation obtained above, the average concentrations detected using Fc-ECG/CuNPs/GE and Fc-ECG/CoNPs/GE were 1.38 and 1.45 mM, respectively. Standard addition method was carried out for recovery study on two prepared sensors. Glucose injection added with 1.70, 2.00 and 2.30 mM glucose was used for Fc-ECG/CuNPs/GE testing and 1.60, 2.00, 2.30 mM glucose injection were added for Fc-ECG/CuNPs/GE

© 2022 The Author(s). Published by the Royal Society of Chemistry

Open Access Article. Published on 10 February 2022. Downloaded on 2/15/2026 8:42:09 PM.
This article is licensed under a Creative Commons Attribution-NonCommercial 3.0 Unported Licence.

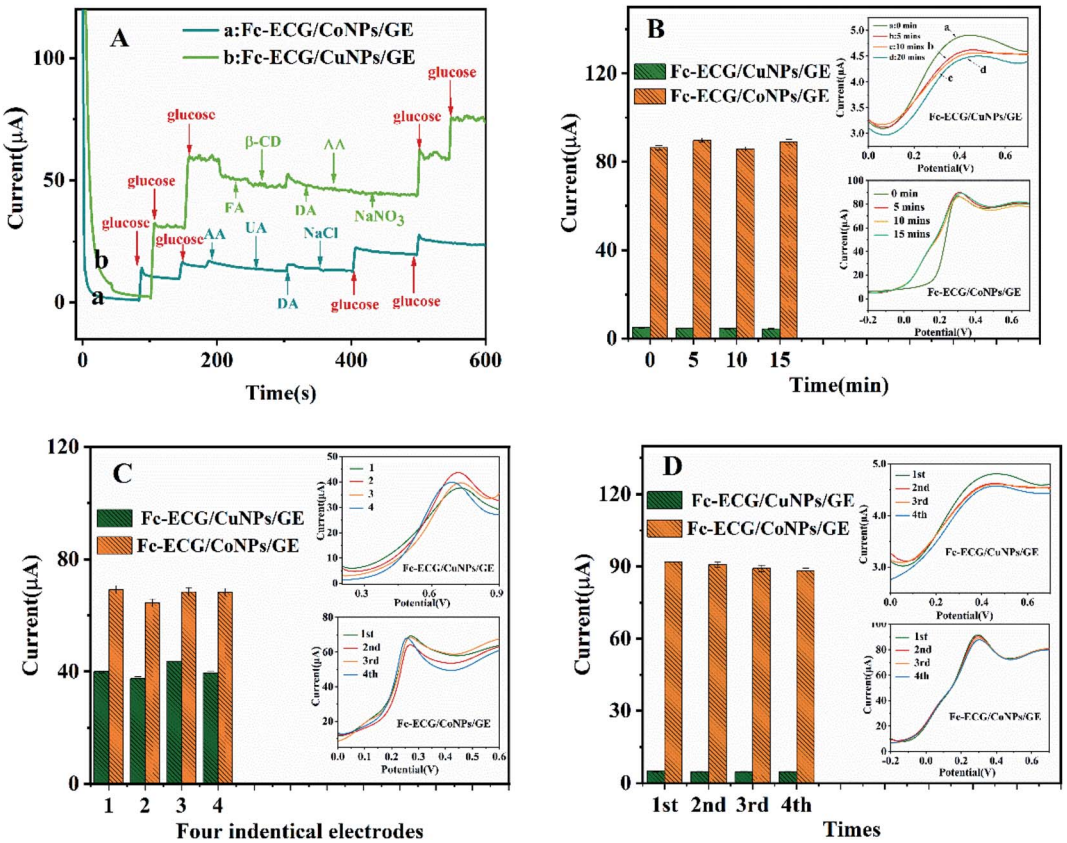

Fig. 3 (A) Selectivity of Fc-ECG/CuNPs/GE (b) and Fc-ECG/CoNPs/GE (a) in the presence of interfering substances by *i*–*t* measurements; (B) stability studies of Fc-ECG/CuNPs/GE and Fc-ECG/CoNPs/GE in the presence of 0.4 and 3.6 mM glucose, respectively (the insets are the DPV responses); (C) repeatability studies of Fc-ECG/CuNPs/GE and Fc-ECG/CoNPs/GE by using 4 different preparations of the same electrodes in the presence of glucose (the insets are the DPV responses); (D) reproducibility studies of Fc-ECG/CuNPs/GE and Fc-ECG/CoNPs/GE by measuring 4 times (the insets are the DPV responses).

Table 2 Detection of glucose in glucose injection samples ($n = 3$)

Added glucose (mM)	Measured current (μA)		Concentration founded (mM)		Recovery (%)		RSD (%)	
	a[a]	b[a]	a[a]	b[a]	a[a]	b[a]	a[a]	b[a]
	23.54	30.42						
0	22.67	30.42	1.38 ± 0.04	1.45 ± 0.01	—	—	2.61	0.40
	22.38	30.26						
	30.52	37.35						
1.70(a)/1.60 (b)	29.83	37.09	1.83 ± 0.17	1.71 ± 0.10	107.65	106.88	6.44	0.58
2	27.13	36.91						
	31.61	45.01						
2.00	31.26	44.18	2.00 ± 0.14	2.00 ± 0.03	100.00	100.00	2.40	0.77
	30.22	44.45						
	34.22	50.43						
2.30	32.03	49.65	2.01 ± 0.11	2.30 ± 0.15	87.39	100.00	5.11	1.38
	31.13	49.00						

[a] a: Fc-ECG/CuNPs/GE; b: Fc-ECG/CoNPs/GE.

testing. According to the experimental data listed in Table 2, the recovery rate of Fc-ECG/CuNPs/GE was between 87.39 and 107.65% while that of Fc-ECG/CoNPs/GE was between 100.00 and 106.88%, suggesting the potential practical application of Fc-ECG/CoNPs/GE as expected.

© 2022 The Author(s). Published by the Royal Society of Chemistry

Open Access Article. Published on 10 February 2022. Downloaded on 2/15/2026 8:42:09 PM.
This article is licensed under a Creative Commons Attribution-NonCommercial 3.0 Unported Licence.

4. Conclusions

In this contribution, the construction of two simple enzyme-free glucose sensors was described, in which gold electrodes were modified with CuNPs and CoNPs followed by drop-casting of the ferrocene-peptide Fc-ECG as redox mediator. The two sensor surfaces exhibit high catalytic activity for glucose oxidation allowing the quantification of glucose over a large linear range, providing excellent stability, repeatability, reproducibility, selectivity, and sensitivity, making them potentially useful for the determination of glucose in blood.

Author contributions

Tao Zhan: development and optimization of electrochemical sensors and real sample analysis, writing – original draft. Xiao-Zhen Feng: supervision, writing and editing. Qi-Qi An: conceptualization, editing and real sample collections. Shiyong Li: conceptualization, editing and real sample collections. Mingyue Xue: supervision, writing and editing. Zhencheng Chen: supervision and review, Guo-Cheng Han: conceptualization, review, and supervision. Heinz-Bernhard Kraatz: supervision, review.

Conflicts of interest

Authors declare no competing financial interests.

Acknowledgements

We appreciate the financial assistance provided from the National Natural Science Foundation of China (No. 81873913, 61861010, 61661014, 61627807), the Nature Science Foundation of Guangxi Province (No. 2018GXNSFAA281198, 2018GXNSFBA281135), and finally Guangxi One Thousand Young and Middle-aged College and University Backbone Teachers Cultivation Program. Financial support from NSERC is acknowledged.

References

1 *WHO, Global report on diabetes*, World Health Organization, Geneva, 2016.
2 S. Wild, G. Roglic, A. Green, R. Sicree and H. King, *Diabetes Care*, 2004, **27**, 1047–1053, DOI: 10.2337/diacare.27.5.1047.
3 H. Teymourian, A. Barfidokht and J. Wang, *Chem. Soc. Rev.*, 2020, **49**, 7671–7709, DOI: 10.1039/d0cs00304b.
4 L. C. Clark Jr and C. Lyons, *Ann. N. Y. Acad. Sci.*, 1962, **102**, 29–45, DOI: 10.1111/j.1749-6632.1962.tb13623.x.
5 M. Adeel, M. M. Rahman, I. Caligiuri, V. Canzonieri, F. Rizzolio and S. Daniele, *Biosens. Bioelectron.*, 2020, **165**, 112331, DOI: 10.1016/j.bios.2020.112331.
6 M. H. Hassan, C. Vyas, B. Grieve and P. Bartolo, *Sensors*, 2021, **21**, 4672, DOI: 10.3390/s21144672.
7 A. E. Cass, G. Davis, G. D. Francis, H. A. Hill, W. J. Aston, I. J. Higgins, E. V. Plotkin, L. D. Scott and A. P. Turner, *Anal. Chem.*, 1984, **56**, 667–671, DOI: 10.1021/ac00268a018.
8 H. Lee, Y. J. Hong, S. Baik, T. Hyeon and D. H. Kim, *Adv. Healthcare Mater.*, 2018, **7**, e1701150, DOI: 10.1002/adhm.201701150.
9 E. Sehit and Z. Altintas, *Biosens. Bioelectron.*, 2020, **159**, 112165, DOI: 10.1016/j.bios.2020.112165.
10 D. W. Hwang, S. Lee, M. Seo and T. D. Chung, *Anal. Chim. Acta*, 2018, **1033**, 1–34, DOI: 10.1016/j.aca.2018.05.051.
11 V. B. Juska and M. E. Pemble, *Sensors*, 2020, **20**, 6013, DOI: 10.3390/s20216013.
12 Z. Zhao, Q. Li, Y. Sun, C. Zhao, Z. Guo, W. Gong, J. Hu and Y. Chen, *Sens. Actuators, B*, 2021, **345**, 130379, DOI: 10.1016/j.snb.2021.130379.
13 K. Shim, W.-C. Lee, M.-S. Park, M. Shahabuddin, Y. Yamauchi, M. S. A. Hossain, Y.-B. Shim and J. H. Kim, *Sens. Actuators, B*, 2019, **278**, 88–96, DOI: 10.1016/j.snb.2018.09.048.
14 F. Zhou, C. You, Q. Wang, Y. Chen, Z. Wang, Z. Zeng, X. Sun, K. Huang and X. Xiong, *J. Electroanal. Chem.*, 2020, **876**, 114477, DOI: 10.1016/j.jelechem.2020.114477.
15 L. Tang, K. Huan, D. Deng, L. Han, Z. Zeng and L. Luo, *Colloids Surf., B*, 2020, **188**, 110797, DOI: 10.1016/j.colsurfb.2020.110797.
16 Z. Lotfi, M. B. Gholivand and M. Shamsipur, *Anal. Biochem.*, 2021, **616**, 114062, DOI: 10.1016/j.ab.2020.114062.
17 K. Tian, K. Baskaran and A. Tiwari, *Vacuum*, 2018, **155**, 696–701, DOI: 10.1016/j.vacuum.2018.06.060.
18 Q. Dong, H. Ryu and Y. Lei, *Electrochim. Acta*, 2021, **370**, 137744, DOI: 10.1016/j.electacta.2021.137744.
19 D. B. Gorle, S. Ponnada, M. S. Kiai, K. K. Nair, A. Nowduri, H. C. Swart, E. H. Ang and K. K. Nanda, *J. Mater. Chem. B*, 2021, **9**, 7927–7954, DOI: 10.1039/d1tb01403j.
20 Y. Gao, C. Zhang, Y. Yang, N. Yang, S. Lu, T. You and P. Yin, *J. Alloys Compd.*, 2021, **863**, 158758, DOI: 10.1016/j.jallcom.2021.158758.
21 J. Zhao, C. Zheng, J. Gao, J. Gui, L. Deng, Y. Wang and R. Xu, *Sens. Actuators, B*, 2021, **347**, 130653, DOI: 10.1016/j.snb.2021.130653.
22 L. Goodnight, D. Butler, T. Xia and A. Ebrahimi, *Biosensors*, 2021, **11**, 409, DOI: 10.3390/bios11110409.
23 Y. J. Hong, H. Lee, J. Kim, M. Lee, H. J. Choi, T. Hyeon and D.-H. Kim, *Adv. Funct. Mater.*, 2018, **28**, 1805754, DOI: 10.1002/adfm.201805754.
24 S. D. Waniek, J. Klett, C. Forster and K. Heinze, *Beilstein J. Org. Chem.*, 2018, **14**, 1004–1015, DOI: 10.3762/bjoc.14.86.
25 P. Mondol and C. J. Barile, *ACS Appl. Energy Mater.*, 2021, **4**, 9611–9617, DOI: 10.1021/acsaem.1c01753.
26 C. Baldoli, L. Falciola, E. Licandro, S. Maiorana, P. Mussini, P. Ramani, C. Rigamonti and G. Zinzalla, *J. Organomet. Chem.*, 2004, **689**, 4791–4802, DOI: 10.1016/j.jorganchem.2004.09.049.
27 D. A. Henckel, M. J. Enright, N. Panahpour Eslami, D. M. Kroupa, D. R. Gamelin and B. M. Cossairt, *Nano Lett.*, 2020, **20**, 2620–2624, DOI: 10.1021/acs.nanolett.0c00162.
28 Y. Peng, Y.-N. Liu and F. Zhou, *Electroanalysis*, 2009, **21**, 1848–1854, DOI: 10.1002/elan.200904601.

© 2022 The Author(s). Published by the Royal Society of Chemistry

Open Access Article. Published on 10 February 2022. Downloaded on 2/15/2026 8:42:09 PM.
This article is licensed under a Creative Commons Attribution-NonCommercial 3.0 Unported Licence.

29 G.-C. Han, A. Ferranco, X.-Z. Feng, Z. Chen and H.-B. Kraatz, *Eur. J. Inorg. Chem.*, 2014, **2014**, 5337–5347, DOI: 10.1002/ejic.201402470.
30 Y.-Y. Cheng, T. Zhan, X.-Z. Feng and G.-C. Han, *J. Electroanal. Chem.*, 2021, **895**, 115417, DOI: 10.1016/j.jelechem.2021.115417.
31 G.-C. Han, X. Su, J. Hou, A. Ferranco, X.-Z. Feng, R. Zeng, Z. Chen and H.-B. Kraatz, *Sens. Actuators, B*, 2019, **282**, 130–136, DOI: 10.1016/j.snb.2018.11.042.
32 M. Saleem, H. Yu, L. Wang, A. Zain ul, H. Khalid, M. Akram, N. M. Abbasi and J. Huang, *Anal. Chim. Acta*, 2015, **876**, 9–25, DOI: 10.1016/j.aca.2015.01.012.
33 S. Malhotra, Y. Tang and P. K. Varshney, *Chem. Pap.*, 2019, **73**, 1987–1996, DOI: 10.1007/s11696-019-00752-7.
34 I. I. Suni, *TrAC, Trends Anal. Chem.*, 2008, **27**, 604–611, DOI: 10.1016/j.trac.2008.03.012.
35 W. Su, Y. Fu, T. Wang, Y. Yu and J. Hu, *RSC Adv.*, 2015, **5**, 79178–79183, DOI: 10.1039/c5ra14313f.
36 X.-Z. Feng, A. Ferranco, X. Su, Z. Chen, Z. Jiang and G.-C. Han, *Sensors*, 2019, **19**, 268, DOI: 10.3390/s19020268.
37 S.-H. Su, H. Cheng and P.-Y. Chen, *J. Chin. Chem. Soc.*, 2013, **60**, 1380–1386, DOI: 10.1002/jccs.201300301.
38 H. Al-Sagur, K. S. Sundaram, E. N. Kaya, M. Durmus, T. V. Basova and A. Hassan, *Biosens. Bioelectron.*, 2019, **139**, 111323, DOI: 10.1016/j.bios.2019.111323.
39 H. Al-Sagur, S. Komathi, M. A. Khan, A. G. Gurek and A. Hassan, *Biosens. Bioelectron.*, 2017, **92**, 638–645, DOI: 10.1016/j.bios.2016.10.038.
40 Y. Zhao, Y. Li, Z. He and Z. Yan, *RSC Adv.*, 2013, **3**, 2178–2181, DOI: 10.1039/c2ra22654e.
41 L. Tang, K. Huan, D. Deng, L. Han, Z. Zeng and L. Luo, *Colloids Surf., B*, 2020, **188**, 110797, DOI: 10.1016/j.colsurfb.2020.110797.
42 Z. Zhao, Q. Li, Y. Sun, C. Zhao, Z. Guo, W. Gong, J. Hu and Y. Chen, *Sens. Actuators, B*, 2021, **345**, 130379, DOI: 10.1016/j.snb.2021.130379.
43 Z. Zhao, Y. Sun, J. Song, Y. Li, Y. Xie, H. Cui, W. Gong, J. Hu and Y. Chen, *Sens. Actuators, B*, 2021, **326**, 128811, DOI: 10.1016/j.snb.2020.128811.

© 2022 The Author(s). Published by the Royal Society of Chemistry